# Optimal operation of a combined cooling system ⋆

**Juan Miguel Serrano** * **Juan D. Gil** ** **Javier Bonilla** *
**Patricia Palenzuela** * **Lidia Roca** *

* *CIEMAT-Plataforma Solar de Almería-CIESOL, Ctra. de Senés km 4.5, 04200 Tabernas, España*
** *CIESOL, Universidad de Almería, Ctra. Sacramento s/n, 04120, Almería, España*

**Abstract:** The effectiveness of Concentrated Solar Power (CSP) plants is significantly influenced by the temperatures at which steam condensation occurs. The existing cooling systems, whether wet (water-cooled) or dry (air-cooled), involve trade-offs. Wet cooling enhances performance but raises concerns due to substantial water usage, particularly in water-scarce regions where CSP plants are often located. On the other hand, dry cooling conserves water but at the cost of reduced efficiency, especially during high ambient temperatures that coincide with peak electricity demand. A possible compromise solution involves a combined cooling system that integrates both wet and dry methods, providing flexibility for overall reduced water consumption and enhanced efficiency.
The incorporation of such systems into CSP plants is thus of great interest, owed to the potential adaptability of its operation to changing conditions. In order to make this optimally and feasible, a suitable control system needs to be developed. In this work we present the first implementation, in a real pilot plant, of a two-layer hierarchical control strategy, where the upper layer solves a multi-objective optimization problem for conflicting water and electricity consumptions, and a regulatory PID-based control layer adapts the system operation to the generated optimal references.

*Keywords:* Process control applications, Optimization, Hierarchical control, Solar energy

## 1. INTRODUCTION

Concentrated Solar Power (CSP) plants use mirrors to concentrate the sun's energy to generate electricity. This technology currently represents a minor part of renewable energy generation: only approximately 5 GW are installed globally. However, the potential for growth is significant given the capability of CSP to provide renewable electricity when needed (thanks to its in-built thermal energy storage), unlike other renewable technologies that are dependent on the availability of the energy source. Another aspect to consider is the ability of these plants to respond to peaks in demand and continue production even in the absence of sunlight, replacing fossil fuel alternatives in managing the grid. According to the International Energy Agency (IEA, 2014) forecasts, CSP has an important potential in the mid to long term, ranging from the 986 TWh by 2030 up to 4186 TWh by 2050, meaning that CSP is forecasted to account for 11 % of global electricity production and 4 % in the case of Europe.

The need to reduce water consumption in these processes (mainly power block cooling) is becoming increasingly evident, especially since they have a wider field of application in areas with significant water scarcity. Added to this is the high price of water, which can be up to 10 €/$m^3$ in such areas (including transportation costs), ultimately calling into question the profitability of this type of application and its sustainability.

Currently, there are two main cooling methods in CSP plants: wet or dry. Wet cooling by evaporative cooling Tower (WCT) is the most common method in CSP plants, since it allows higher efficiencies (as it is based on the wet bulb temperature). However, their main problem is the need for constant resupply of the evaporated water. An example of the large water consumption in wet-cooled CSP plants is the plant located in the Mojave Desert, California, with a consumption of approximately 3 $m^3$/MWh (Damerau et al., 2011), making it environmentally unsustainable. Dry Cooling systems (DC) are based on dry bulb temperature and have hardly any water consumption (between 0.30 and 0.34 $m^3$/MWh Bourillot (1983)). The most widespread DC systems are based on the use of air cooled condensers (ACC), although there are several dry cooling methods, such as "Air Cooler Heat Exchangers (ACHE)". Despite the low water consumption, the main problem of dry cooling systems compared to wet cooling systems is the high investment costs and the significant reduction in electricity production due to the higher condensing temperatures required in the power block (up to 10 % reduction in power output).

⋆ This publication is part of the R&D project PID2021-126452OA-I00, funded by MCIN/ AEI/10.13039/501100011033/ and "ERDF A way of making Europe".

There are different types of innovative cooling systems that can reduce water consumption: those that integrate dry and wet cooling systems in the same cooling device, which are called hybrid cooling systems (Rezaei et al., 2010; Asvapoositkul and Kuansathan, 2014; Hu et al., 2018) and those that combine a dry and a wet cooling system, which are called combined cooling systems. The latter are presented as the most suitable option since their flexible operation enables adaptability depending on environment conditions, allowing the best operating strategies to be selected to achieve a compromise solution between water and electricity consumption. The most common type found in the literature is that which considers an air-cooled condenser (ACC) in parallel with a WCT (Barigozzi et al., 2011, 2014). In this case, the turbine outlet steam is condensed through the ACC and/or through a surface condenser coupled to the WCT. Another configuration, recently proposed in the literature (Palenzuela et al., 2022a) is the combination of a wet and a dry cooling tower (ACHE type), both sharing a surface condenser. In this case, the steam is condensed through the surface condenser and the cooling water at the outlet (at higher temperature) is cooled either through the WCT or through the DC, or different combinations of both.

This potential adaptability can only be realized if a suitable control system is set in place. In this work we present the development and implementation of a complete control solution in an experimental pilot plant, it is a two-layer hierarchical control architecture that, on-line, evaluates and selects the optimal operation strategy, given some operation conditions and selection criteria, and regulates the pilot system inputs to achieve it.

## 2. COMBINED COOLING SYSTEM

The combined cooling pilot plant at the Plataforma Solar de Almería (see Fig.1) consists in three circuits: cooling circuit, exchange circuit and heating circuit. In the cooling circuit, water circulating inside the tube bundle of a Surface Condenser (whose thermal power at nominal conditions is 80 $kW_{th}$ ) is cooled through a WCT and/or a DC (type ACHE), both with a thermal power at design conditions of 204 $kW_{th}$ . Valves 1 and 2 ($V_1$, $V_2$) allow the operation in different configurations: only DC ($V_1$=$V_2$=II), only WCT ($V_2$=I), in series ($V_1$=I, $V_2$=II), in parallel with different aperture percentages ($V_1$=II, $V_2$ between I and II) or parallel-series with different aperture percentages ($V_1$ and $V_2$ between I and II). In the exchange circuit, a saturated steam generator with 80 $kW_{th}$ of thermal power at nominal conditions, generates steam at different pressures (ranging between 82 and 200 mbar), that is in turn condensed through the Surface Condenser, transferring its latent heat to the cooling water that is thus heated. Finally, in the heating circuit, a 300 $kW_{th}$ static solar field provides the thermal energy required by the steam generator using hot water as the heat transfer fluid. A more detailed description can be found in (Palenzuela et al., 2022a).

### *2.1 Experimental campaigns*

For the modeling of the combined cooling system, a data base of experimental results has been used. Those results are based in an experimental campaign described in Palenzuela et al. (2022a) and two more campaigns that were designed to characterize the two cooling systems (DC and WCT) in a wide range of ambient and operating conditions. In the case of the DC, an experimental campaign based on a *Box-Behnken* design with four factors has been used. For the WCT, a factorial design with two leves and five variables has been selected. Table 1 shows the range of variation of the variables involved, considering all the experimental campaigns performed.

In the case of the control strategy, an experimental campaign has been carried out to identify First Order Plus Dead Time (FOPDT) transfer functions, such as described in Section 4.1 and evaluate the low level controllers. In addition, the performance of whole hierarchical control system has been evaluated during the last experimental campaign performed at the pilot plant in the winter 2023 as shown in Section 6.

## 3. CONTROL PROBLEM DESCRIPTION

The cooling system has to satisfy one primary goal, condensate all incoming saturated vapor into saturated liquid, i.e. meeting the cooling requirements. In order to achieve this, it makes use of two resources: electricity and water. The nature of this process makes it so that both resources have conflicting trends, so it is fundamentally a multi-objective optimization problem. There is no single optimal solution but a collection of good solutions (the Pareto front region, Censor (1977); Gendreau and Potvin (2010)) with trade-offs among the considered objectives: reducing the electricity consumption necessarily comes at the expense of increased water usage, and viceversa.

From the results obtained in (Palenzuela et al., 2022b), it was concluded that the most suitable configuration depends on the operating and ambient conditions, so the control system (see Fig. 2) is tasked with finding out the best operation strategy, on-line during operation, that satisfies the cooling requirements. It is a two layer system where in the upper layer, a multi-objetive optimization is performed, obtaining a range of optimal operation points, the Pareto front. In order to choose from the range of optimal strategies, the chosen criteria was to minimize the electricity consumption while keeping the water consumption below a defined limit. The decision variables obtained are then established as the setpoints of a regulatory PID control layer (lower layer), in charge of manipulating the system actuators.

## 4. MODELING

The model of the combined cooling system (see Figure 3) consists on the combination of the models of its main components: dry cooler, wet cooling tower, surface condenser, pump, three-way valves and the different mixing of fluids that take place.

There are mainly two types of models, on the one hand FOPDT transfer functions have been used to model the dynamic relation between the control variables or actuators and the controlled variables. On the other hand a combination of first principle and black-box modeling approaches was used to evaluate the behavior of the system

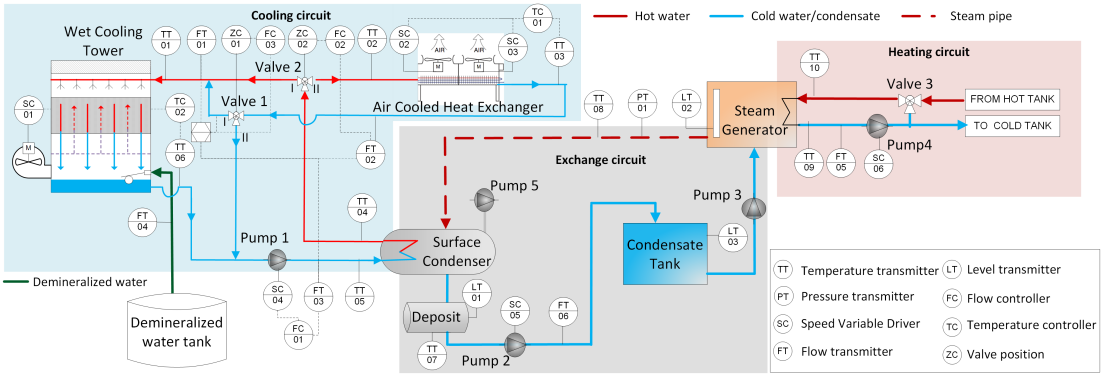


Fig. 1. Layout of the combined cooling pilot plant at PSA

in steady state conditions. This allows to, given some operating conditions, have the ability to predict the cooling capabilities of the combined system and the associated consumptions depending on the chosen operation strategy.

### *4.1 FOPDT models*

The dynamic transfer functions were determined experimentally by means of open-loop tests involving step changes in the actuators. The reaction curve method was employed to extract the parameters of the FOPDT transfer functions. Table 2 presents the transfer functions corresponding to the mean operating range of each control variable, with $y$ representing the controlled variables, $u$ the control variables, $K$ the static gain, $\tau$ the time constant and $d$ the time delay. This was done for the DC and WCT, the surface condenser pump and both three-way valves $V_1$ and $V_2$.

### *4.2 Steady state models*

*Dry cooler* The model of the DC (see Fig. 3 - *DC*) is a black-box model based on Artificial Neural Network (ANN). Concretely, it is a ANN model multi-layer non-recurrent, so its application is limited to systems with the same characteristics (in terms of configuration and dimensions) as the studied system within the operation range considered (see Table 1). The output of the model is the temperature of the cooling water leaving the DC, $T_{dc,out}$ and the input variables are: the cooling water flow rate circulating through the DC ($q_{dc}$), the cooling water temperature at the inlet of the DC ($T_{dc,in}$), the fans frequency ($\omega_{dc}$) and the ambient temperature ($T_{amb}$). Another output variable is the electrical consumption, $C_{dc,e}$, that has been modeled by a parametric adjustment from experimental data that relate this variable $\omega_{dc}$.

*Wet cooling tower* The model of the WCT (see Fig. 3 - *DC*) is also based on ANN, same type of the DC. In this case, the output variables are: the cooling water temperature at the outlet of the WCT, $T_{wct,out}$, and the water consumption due to evaporation and drift losses, $C_w$. The input variables are: the cooling water flow rate circulating through the WCT ($q_{wct}$), the cooling water temperature at the inlet of the WCT ($T_{wct,in}$), the fan frequency ($\omega_{wct}$) the ambient temperature ($T_{amb}$) and the relative humidity ($\phi$). As in the case of the DC, the electrical consumption, $C_{wct,e}$, has been modeled by a

Table 1. Range of variation of the input and output variables

| Variable | Range |
|---|---|
| Ambient temperature, $T_{amb}$ | 9-39 °C |
| Relative humidity, $\phi$ | 10-89 % |
| Water flow rate in DC, $q_{dc}$ | 5-24 $m^3/h$ |
| Water flow rate in WCT, $q_{wct}$ | 6-24 $m^3/h$ |
| Water consumption in WCT, $C_w$ | 53-332 l/h |
| Water temperature at the DC inlet, $T_{dc,in}$ | 33-42 °C |
| Water temperature at the WCT inlet, $T_{wct,in}$ | 31-41 °C |
| Water temperature at the DC outlet, $T_{dc,out}$ | 29-38 °C |
| Water temperature at the WCT outlet, $T_{wct,out}$ | 22-34 °C |
| Variable frequency drive of the DC fans, $\omega_{dc}$ | 11-99 % |
| Variable frequency drive of the WCT fan, $\omega_{wct}$ | 21-93 % |

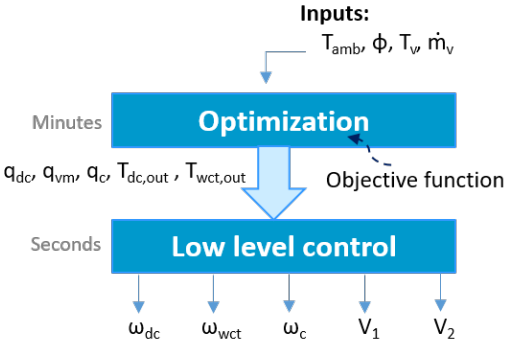


Fig. 2. Control structure

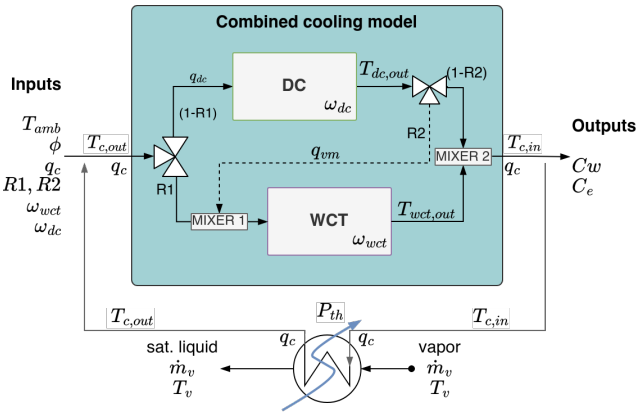


Fig. 3. Complete system model diagram

Table 2. Transfer functions experimentally obtained

| System | $y$ | $u$ | $K$ | $\tau$ (s) | $d$ (s) |
|---|---|---|---|---|---|
| DC | $T_{dc,out}$ | $\omega_{dc}$ | -0.16 ° C/% | 47.7 | 26.7 |
| WCT | $T_{wct,out}$ | $\omega_{wct}$ | -0.12 ° C/% | 49.6 | 34.4 |
| Pump 1 | $q_c$ | $\omega_c$ | 0.25 $m^3$/( h·%) | 2 | 1 |
| Valve 2 | $q_{dc}$ | $V_2$ | -3.1 $m^3$/( h·%) | 2 | 1 |
| Valve 1 | $q_{vm}$ | $V_1$ | 0.99 $m^3$/( h·%) | 5 | 1 |

parametric adjustment with experimental data that relate this variable with $\omega_{wct}$.

*Surface condenser* The surface condenser (see Figure 3 - *SC*) was modeled by applying an energy balance, where it is assumed that all the vapor that enters the condenser (at saturated conditions), leaves it as saturated liquid, so the outlet temperature from the cooling water can be estimated as:

$$T_{c,out} = T_{c,in} + \frac{\dot{m}_v \lambda_{sat,v}(T_v)}{\dot{m}_c c_p(T_{c,in}, P_c)} , \quad (1)$$

where $T_{c,in}$ and $T_{c,out}$, are the cooling water inlet and outlet temperatures, respectively, $\dot{m}_c$, the cooling water mass flow rate, $T_v$, vapour temperature and $\dot{m}_v$ its mass flow rate. Finally $\lambda_{sat,v}$, is the phase change enthalpy of the saturated vapour and $c_p$, the specific heat.

*Mixers* The mixers outlet flow ($q_{mix,out,i}$) and temperature ($T_{mix,out,i}$) can be determined with a simple mass and energy balances from its inlets streams ($q_{mix.in}$, $T_{mix.in}$):

$$q_{mix,out,i} = q_{mix,in,1} + q_{mix,in,2} , \quad (2)$$

$$T_{mix,out,i} = T_{mix,in,1} \cdot \frac{c_p(T_{mix,in,1})}{c_p(T_{out,i})} \frac{q_{mix,in,1}}{q_{mix,out,i}} + T_{mix,in,2} \cdot \frac{c_p(T_{mix,in,2})}{c_p(T_{out,i})} \frac{q_{mix,in,2}}{q_{mix,out,i}} , \quad (3)$$

where $c_p$ is the specific heat, which can be assumed to be the same for the mixing temperature differences of this type of system.

As mentioned above, the complete system model (combined cooling + surface condenser) is obtained by combining the above component models. The resulting system exhibits a highly non-linear response to changes in its inputs, as well as discontinuities resulting from the activation or deactivation of individual components (DC and WCT).

## 5. CONTROL

### *5.1 Low-level control layer*

It is a regulatory layer including five control loops, as described in Table 3. The objective of this layer consists on tracking the setpoints calculated by the upper layer for the five controlled variables and maintaining them near steady state conditions around these references, even in the presence of disturbances such as variations in temperature or flow rate.

Classical feedback loops with PI controllers have been used in this regulatory layer, which were tuned using the improved SIMC technique Skogestad and Grimholt (2012) according to the models presented in Table 2 and considering a close-loop time constant between 1 and 1.4 times the constant time of the systems, depending on the PI controller. Table 3 summarizes the proportional gain, $K_p$, and the integral time, $T_i$, for each control loop. The ideal configuration of the PI controller has been implemented, $C(s) = K_p(1 + 1/(T_i s))$, including anti-windup mechanism and sample time of 1 s.

### *5.2 Optimization layer*

The aim of the optimization is to satisfy the operation requirements, thus guaranteeing the cooling thermal power needed according to the ambient conditions (ambient temperature and humidity) and resources restrictions (water).

The cost function to evaluate the performance of the system is described in Eqs. (4),(5):

$$\min_u J(C_w, C_e) = f(T_{amb}, \phi, q_c, R_1, R_2, \omega_{dc}, \omega_{wct}), \quad (4)$$

$$s.t. \, C_w \leq C_{w,max}, u_{min} \leq u \leq u_{max}, \quad (5)$$

where, as shown in Fig. 3, $C_w$ and $C_e$ are the water and electricity consumptions, respectively; $u$ represents the inputs: $R_1$ being the ratio of $q_c$ that, in parallel, goes towards the WCT, while $R_2$ the ratio of $q_{dc}$ that, in series, circulates through the WCT. Finally, $\omega_{dc}$ and $\omega_{wct}$ are the fan speed of each component. When a feasible solution is found, it is immediate to calculate the optimal setpoints to be given to the regulatory layer [1] ($T^*_{dc,out}$, $T^*_{wct,out}$, $q^*_c$, $q^*_{dc}$, $q^*_{vm}$).

The problem is solved by means of a Genetic algorithm (GA). GAs represent a powerful class of optimization techniques widely employed in solving complex problems, where highly non-linear and discontinuos models, as the one of this work, are used. GAs evolve a population of candidate solutions iteratively. The algorithm begins by initializing a population, where partial initialization is provided by previous optimization runs, with subsequent iterations involving the selection of elite individuals based on their fitness values. This process incorporates tournament selection to choose parents for crossover and mutation operations, allowing the generation of diverse offspring in an attempt to avoid getting trapped in local minimums. GAs, such as the implemented in this work employing MATLAB's *gamultiobj* (MATLAB (2023)), implements a variant of NSGA-II (Deb, 2011)), that prioritizes elitism by favoring individuals with superior fitness while also valuing diversity, thus striking a balance between exploration and exploitation. This iterative process continues until a predefined running time elapses (established in 300 seconds in this case).

Tuning of this metaheuristic algorithm parameters is a very important aspect of the implementation which needs to be fitted ad-hoc. This has been done systematically by selecting three case studies and evaluating 4 different

[1] The superscript * indicates a decision variable from the optimization layer, a setpoint for the low-level control layer

Table 3. Low-level control loops

| Controller | Control signal variable | Control signal P&ID | Controlled signal variable | Controlled signal P&ID | $K_p$ | $T_i$ (s) |
|---|---|---|---|---|---|---|
| TC-01 | $\omega_{dc}$ | SC-02, SC-03 | $T_{dc,out}$ | TT-03 | -4.5 %/°C | 56.6 |
| TC-02 | $\omega_{wct}$ | SC-01 | $T_{wct,out}$ | TT-06 | -5.9 %/°C | 61.1 |
| FC-01 | $\omega_c$ | SC-04 | $q_c$ | FT-06 | 2.3 %·($h$·m$^3$) | 2.5 |
| FC-02 | $V_2$ | ZC-02 | $q_{dc}$ | FT-02 | -0.2 %·$h$·m$^{-3}$ | 2.3 |
| FC-03 | $V_1$ | ZC-01 | $q_{vm}$ | $f$(FT-01,FT-02, FT-03) | 0.7 %·$h$·m$^{-3}$ | 5.0 |

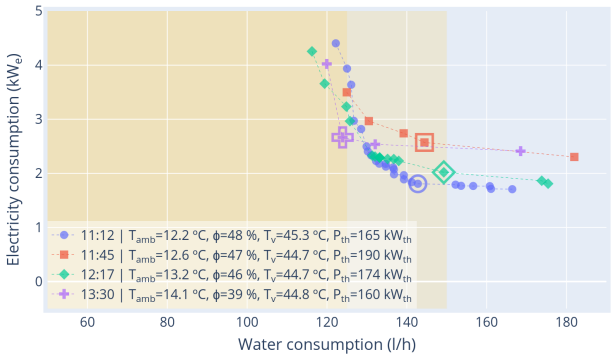


Fig. 4. Pareto fronts for each case study with highlighted selected optimum

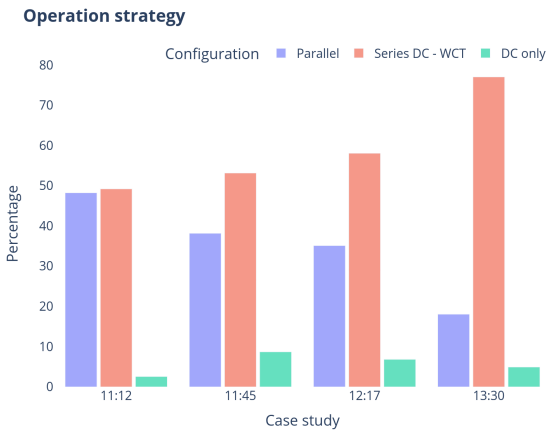


Fig. 5. Different operation configurations obtained in the evaluations

parameters: population size, elite set size ratio, crossover fraction and tournament size ratio (Grygar and Fabricius, 2019). Finding that, in general, the best values for this particular problem are 200, 0.1, 0.8 and 2, respectively. The parameters are changed depending on the scenario, when the optimization is run for the first time with no prior knowledge, the population size is increased up to 250, and given more time to try to find a good first pareto estimation, while when subsequent iterations are evaluated, partial initialization is used taking prior solutions, and this time, the crossover fraction is decreased to 0.5, this increases the mutation rate instead of crossover to favour exploration of the solution space.

## 6. RESULTS

The experimental results from the application of the proposed methodology are shown in Fig. 6. The first group of three figures contains information relevant to the optimization layer, while the ten remaining figures represent the control layer. The optimization layer is evaluated 11 times by calculating the mean of the last 300 samples (5 minutes) with the condition that the system is stable (mainly cooling requirements). Every time the optimization layer is processed, updated optimal setpoints are generated for the control layer.

In general, solid lines represent the experimental values recorded with the data acquisition system, a dash-dotted line ($-\cdot-$) indicates a variable from the optimization layer, either a given input (e.g. $T_{amb}$) or internal evaluations (e.g. $C_e$). In the case of the control layer plots, the optimizer outputs are the setpoints for the control layer and they are represented with a dashed line ($--$).

The objective of the test was to validate experimentally the hierarchical control scheme given real operating conditions, so a evaluation of the optimization layer is performed every time the environment variables (Fig.6 - *Environment* - $T_{amb}$, $\phi$) drift significantly, and/or when the cooling requirements were changed. Thermal power requirements (Fig.6 - *Cooling requirements* - $P_{th}$) vary depending on the vapour temperature ($T_v$) and/or vapour mass flow rate ($\dot{m}_v$, not included in the figure for simplicity). For each optimization a prediction of the expected consumptions to be obtained, after a transitory period, is shown in terms of electricity ($C_e$) and water ($C_w$) together with the experimentally obtained values (Fig.6 - *Costs*).

The multi-objective optimization solution for 4 of the 11 cases evaluated are shown in Fig. 4, highlighting the chosen solution for each evaluation. For this particular test, the ambient conditions did not change significantly over the test duration, thermal power requirements started at a lower value of 165 kW for the first considered evaluation (at 11:12), raised to 190 kW for the second at 11:45, returned to a lower value of 174 kW half an hour later (12:17), and maintained there for a longer period. Finally, after about an hour (13:30) similar ambient conditions were observed and cooling conditions were kept low (160 kW) in the last evaluation. The selection criteria was the same for all runs, except for the last one, where the maximum water consumption criteria was lowered from 150 to 125 l/h.

From the qualitative analysis of the results five main takeaways can be taken:

(1) Analyzing how the operation strategy is modified to adapt to the changing conditions or selection criteria (Fig. 5), it can be seen that for the first evaluation (11:12) the strategy is a mix of parallel and series operation. This configuration is maintained when increasing the thermal load (11:45), but with an increase in the cooling flow ($q_c$). Later, when return-

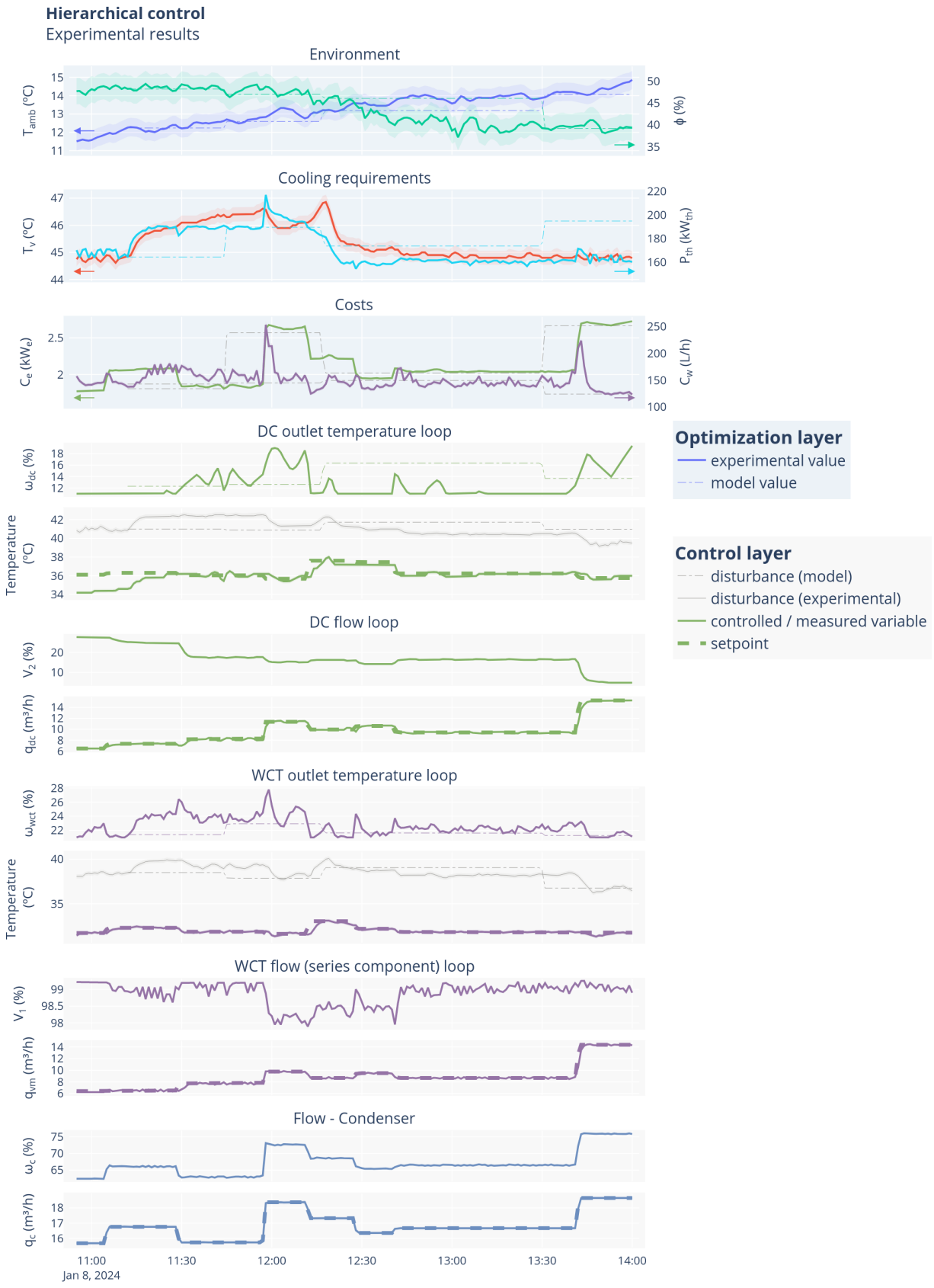


Fig. 6. Experimental results of proposed methodology

ing to the first evaluation cooling requirements and not significant changes in the environmental conditions (12:17), as expected the chosen solution yields very similar configuration and consumptions. Finally, when increasing the restriction in water consumption (13:30), the optimal strategy shifts towards only series operation while increasing the cooling flow.

(2) The Dry cooler and Wet cooling tower models were validated and produced accurate predictions within the uncertainty limits. However the condenser model is a simple energy balance and, as it can be observed in Fig. 6 - *Temperature DC*, there is a significant difference between the expected condenser outlet temperature ($T_{c,out} = T_{dc,in}$) and the experimental value. This is a clear area for improvement.

(3) As it stands, the decision variables were updated at more or less fixed periods of time, or when the cooling requirements were changed and a new stable operation was reached, this was a manual process. The next implementation step should automatize this. As observed, variables may change suddenly and diverge from the last optimization evaluation, thus it seems appropriate to re-evaluate the optimization layer every time one of the system variables drifts by a significant amount. A steady-state identification algorithm could be implemented to make the control sensitive to the changing conditions.

(4) The low-level control requirements of this system are positively satisfied with a simple PID-based control system, managing to reach the established setpoints in a reasonable time. In the case of DC system, the control variable shows some oscillations due to the non-linearities of the model. Next versions will include a Gain Scheduling PID controller to improve the low-level control response.

(5) Providing the GA of the optimization layer with prior solutions from similar operating conditions yields significantly improved results, allowing subsequent optimization runs to start from an already close to optimal solution. This advantage could be extended to, not only using information from a particular test and prior evaluation, but to, overt time, build a database of operation points and select similar evaluations from it.

## ACKNOWLEDGEMENTS

The authors would like to thank the Plataforma Solar de Almería for providing access to its facilities.

## REFERENCES

Asvapoositkul, W. and Kuansathan, M. (2014). Comparative evaluation of hybrid (Dry/Wet) cooling tower performance. *Applied Thermal Engineering*, 71(1), 83–93. doi:10.1016/j.applthermaleng.2014.06.023.

Barigozzi, G., Perdichizzi, A., and Ravelli, S. (2011). Wet and dry cooling systems optimization applied to a modern waste-to-energy cogeneration heat and power plant. *Applied Energy*, 88(4), 1366–1376. doi: 10.1016/j.apenergy.2010.09.023.

Barigozzi, G., Perdichizzi, A., and Ravelli, S. (2014). Performance prediction and optimization of a waste-to-energy cogeneration plant with combined wet and dry cooling system. *Applied Energy*, 115, 65–74. doi: 10.1016/j.apenergy.2013.11.024.

Bourillot, C. (1983). Hypotheses of calculation of the water flow rate evaporated in a wet cooling tower. Place: United States.

Censor, Y. (1977). Pareto optimality in multiobjective problems. *Applied Mathematics and Optimization*, 4(1), 41–59. doi:10.1007/BF01442131.

Damerau, K., Williges, K., Patt, A.G., and Gauché, P. (2011). Costs of reducing water use of concentrating solar power to sustainable levels: Scenarios for North Africa. *Energy Policy*, 39(7), 4391–4398. doi: 10.1016/j.enpol.2011.04.059.

Deb, K. (2011). Multi-objective optimisation using evolutionary algorithms: an introduction. In *Multi-objective evolutionary optimisation for product design and manufacturing*, 3–34. Springer.

Gendreau, M. and Potvin, J.Y. (eds.) (2010). *Handbook of Metaheuristics*, volume 146 of *International Series in Operations Research & Management Science*. Springer US, Boston, MA. doi:10.1007/978-1-4419-1665-5.

Grygar, D. and Fabricius, R. (2019). An Efficient Adjustment of Genetic Algorithm for Pareto Front Determination. *Transportation Research Procedia*, 40, 1335–1342. doi:10.1016/j.trpro.2019.07.185.

Hu, H., Li, Z., Jiang, Y., and Du, X. (2018). Thermodynamic characteristics of thermal power plant with hybrid (Dry/Wet) cooling system. *Energy*, 147, 729–741. doi:10.1016/j.energy.2018.01.074.

IEA (2014). Energy Technology Perspectives.

MATLAB (2023). gamultiobj Algorithm - MATLAB & Simulink - MathWorks España.

Palenzuela, P., Roca, L., Asfand, F., and Patchigolla, K. (2022a). Experimental assessment of a pilot scale hybrid cooling system for water consumption reduction in CSP plants. *Energy*, 242, 122948. doi: 10.1016/j.energy.2021.122948.

Palenzuela, P., Roca, L., Asfand, F., and Patchigolla, K. (2022b). Experimental assessment of a pilot scale hybrid cooling system for water consumption reduction in CSP plants. *Energy*, 242, 122948. doi: 10.1016/j.energy.2021.122948.

Rezaei, E., Shafiei, S., and Abdollahnezhad, A. (2010). Reducing water consumption of an industrial plant cooling unit using hybrid cooling tower. *Energy Conversion and Management*, 51(2), 311–319. doi: 10.1016/j.enconman.2009.09.027.

Skogestad, S. and Grimholt, C. (2012). The SIMC Method for Smooth PID Controller Tuning. In R. Vilanova and A. Visioli (eds.), *PID Control in the Third Millennium: Lessons Learned and New Approaches*, Advances in Industrial Control, 147–175. Springer, London. doi: 10.1007/978-1-4471-2425-$2_5$.